# Precise luminosity measurement at a Linear Collider

S. Lukić*

Vinča Institute of Nuclear Sciences, University of Belgrade, Serbia

On behalf of the FCAL Collaboration

**Abstract**

The high charge density and high energy at future linear colliders will present challenges to the luminosity measurement that have not been there in the past. The intense electromagnetic interaction between the electron bunches influences the luminosity measurement at the level of several percent. Precise correction of the beam-beam effects, based on experimentally measurable quantities, is described here. In addition, a comprehensive list of systematic effects in luminosity measurement is given, with their individual contributions to the final uncertainty of the luminosity figure.

# 1 Introduction

High-precision capabilities of linear electron-positron colliders earn such experiments a significant place in the program of elementary particle physics. A crucial condition necessary to fully realize the precision potential of the linear colliders is precise measurement of luminosity. Luminosity is a key figure relating the observed number of events of a given process to its cross section. In the most straightforward sense, it can be defined by the expression,

$$L = N_1 N_2 \frac{f}{A} \tag{1}$$

*E-mail:slukic@vinca.rs

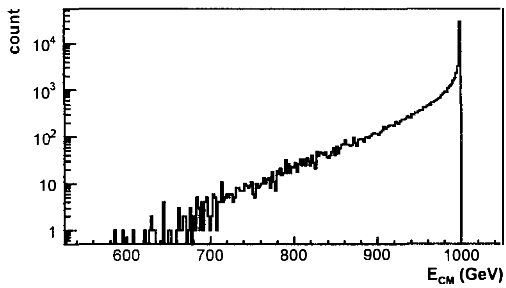


Figure 1: Luminosity spectrum at 1 TeV ILC, simulated using Guinea-Pig [1]

Here $N_1$ and $N_2$ are the average populations of the colliding bunches, $f$ is the overall bunch-crossing rate, and $A$ is the overlap integral of the 2D density distributions of the two bunches in the perpendicular plane.

The *luminosity spectrum* $\mathcal{L}(E_{CM})$ is defined as the distribution of the center-of-mass (CM) energy $E_{CM}$ available to individual collisions in the experiment. Due to beam-beam effects (see Sec. 2), the luminosity spectrum features the characteristic low-energy tail (Fig. 1)

The basic expression,

$$L\sigma_a = N_a \tag{2}$$

relates the luminosity, the cross section $\sigma_a$ of an elementary process $a$ in a given part of the phase space defined by experimental selection cuts, and the number of detected events $N_a$ of the process $a$ in the same part of the phase space.

In production threshold scans, the luminosity spectrum, including the luminosity peak shape, as well as the low-energy tail, affect the results of the scan in a considerable way [2]. It is thus indispensable to know the luminosity spectrum to sufficient precision in order to be able to fit the theoretical distributions of the kinematic parameters to the measurement.

Presently the most precise way to measure luminosity at a linear collider is to use Bhabha-scattering as the gauge process. Bhabha scattering is characterized by low angles (the cross section scales approximately with $\theta^{-3}$), as well as by final energies close to the beam energy. The cross section is relatively high, ensuring good statistical accuracy. Precision better than $10^{-3}$ was reached with this method at LEP, thanks to a careful experimental setup, and precise QED calculations [3, 4, 5, 6]. At future linear colliders, the International Linear

Collider (ILC) [7] and the Compact Linear Collider (CLIC) [8], the CM energy will be 3 to 30 times higher, and luminosity up to thousand times higher. In such conditions, intense beam-beam effects induce severe counting biases of Bhabha-events which require dedicated correction procedures, as pointed out in Ref. [9].

## 1.1 The luminosity calorimeter - LumiCal

The luminometer for the future linear colliders (LumiCal, Fig. 2) is designed as a pair of sampling calorimeters with cylindrical geometry, centered around the outgoing beam axis at $\sim 2.5$ m from the interaction point (IP) on both sides. The calorimeters consist of a number of layers in the longitudinal direction, each layer containing a tungsten disk and a segmented sensor plate. Electromagnetic (EM) showers developing in tungsten are sampled in the sensor plates. The absorber plates are each 3.5 mm thick, corresponding to one radiation length in tungsten. The number of layers is 30 for ILC, and 40 for CLIC. The Molière radius of LumiCal is $\sim 1.5$ cm. The sensor plates are segmented both radially and azimuthally, allowing full reconstruction of the four momenta of the detected particles. The outer radius of the LumiCal is 196 mm in the ILC case, and ca. 300 mm in the CLIC case. The inner radius is 80 mm in the ILC case, and 100 mm in the CLIC case.

The fiducial volume (FV) of the calorimeters is defined as the angular range with optimal energy resolution, and covers angles from 41 to 67 mrad at ILC, and 43 to 80 mrad at CLIC.

Bhabha events are recognized by coincident detection of showers in the FV of both halves of the luminometer in a given energy range near the peak energy. According to Eq. 2, the luminosity figure is then obtained by dividing the number of detected events by the Bhabha cross section integrated in the corresponding region of the phase space.

In Sec. 2, the physical processes affecting the luminosity measurement will be outlined, and the event simulation methods used in this work will be briefly described. In Sec. 3, a method of handling the counting bias due to beam-beam effects will be described and tested on simulated events. In the conclusions, the performance of the method for the final precision of the luminosity measurement will be summarized and discussed.

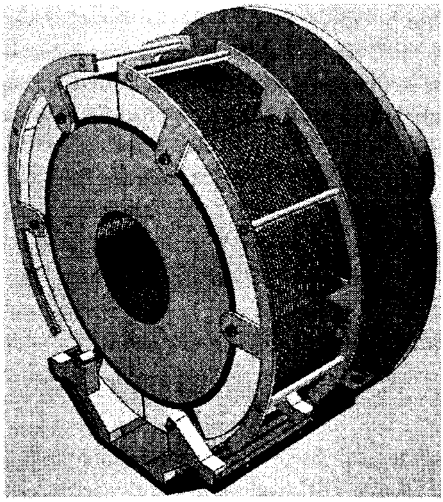

Figure 2: LumiCal sketch

# 2 Physics of the luminosity measurement

## 2.1 Physical processes affecting the luminosity measurement

### Beamstrahlung

In order to reach the projected luminosity at future linear colliders, the electron[1] beams will be focused to a few nm in the vertical direction, and a few ten to few hundred nm in the horizontal directions [7, 8] at the interaction point (IP), resulting in extremely high local charge densities, and extremely intense EM interaction between the opposing bunches. In case of a charge moving with relativistic velocity $\vec{v}$, the component of EM field perpendicular to $\vec{v}$ scales the Lorentz factor $\gamma = 1/\sqrt{1 - v^2/c^2}$. At future linear colliders, the Lorentz factor of the bunches is of the order of $10^6$ in the lab frame, or $10^{12}$ in the rest frame of the opposing bunch. Since the bunches have opposite charge signs, the direction of the perpendicular component of the Lorentz force points towards the bunch center. This results in a very strong focusing effect of the bunches – the *pinch effect*. The pinch effect enhances the luminosity, but induces emission of intense and energetic EM radiation, *Beamstrahlung*, from the electrons in the

[1] Unless stated otherwise, electron always refers to electron or positron

bunch. For an elaborate treatment of the beam-beam effects, see Refs. [10, 1].

The angular distribution of Beamstrahlung is contained in several hundred μrad around the beam axis. The distribution of energy loss of individual electrons is very wide, and depending on the conditions, may reach up to the beam energy. This leads to the creation of the low-energy tail of the luminosity spectrum (see Fig. 1). At the level of individual $e^+e^-$ collision events, Beamstrahlung energy loss prior to the collision is asymmetric between the two colliding particles, resulting in non-zero velocity of the CM frame of the collision with respect to the lab frame.

### Initial and Final State Radiation

The Bhabha process is accompanied by emission of the initial- and final state radiation (ISR, FSR). ISR and FSR are QED phenomena, and their energy- and angular distributions can be precisely calculated [11]. Due to the quantum interference terms, ISR and FSR cannot be cleanly separated at the fundamental level. The resulting angular distribution is quasi-continuous, with sharp peaks around the initial and final electron momenta.

### Boost of the collision frame

In the frame of the two Bhabha electrons after emission of Beamstrahlung and ISR, and before emission of FSR, the *collision frame*[2], the deflection angle is the same for both particles, according to the momentum-conservation principle. This angle is denoted the *scattering angle*, $\theta^{coll}$.

As the collision frame is recoiling against the photons radiated before the scattering, it has a velocity $\vec{\beta}_{coll}$ with respect to the lab frame. $\vec{\beta}_{coll}$ is collinear with the beam axis, axcept in rare cases when ISR is emitted under significant angle with respect to the beam. In the lab frame, the final particles have angles $\theta_1^{lab}$ and $\theta_2^{lab}$, which correspond to the scattering angle $\theta^{coll}$ and its mirror image $\pi - \theta^{coll}$ boosted by $\vec{\beta}_{coll}$. Because of the boost, even if $\theta^{coll}$ was in the angular range of the FV of the LumiCal, one or both of the final angles in the lab frame may be outside FV. In this way, Beamstrahlung induces an *angular counting loss* of Bhabha events.

At LEP, the intensity of the beam-beam effects was small, and application of asymmetric selection cuts was sufficient to minimize the uncertainties arising from the Beamstrahlung to the required level. At future linear colliders, where

[2] Also denoted the *hard-scattering frame* in literature, see [11]

the beam-beam effects are far more intense, the angular counting loss is of the order of several percent. If one endeavors to correct this counting bias using bunch-crossing simulations, the ultimate precision will be limited by the precision of the simulation, and by the uncertainties in the determination of beam parameters. A method of event-by-event correction of the angular counting loss by direct measurement of the boost of the collision frame [12] is described in sec 3.

### Processes after scattering

After scattering, the final electrons may emit FSR. Beside that, their trajectories are deflected inwards by a fraction of mrad under the influence of the EM field of the opposing bunch, thus inducing a small additional angular counting loss termed Electromagnetic Deflection (EMD) effect. Beamstrahlung may be emitted at this stage as well, but since it is emitted under very small angles with respect to the final electrons, it is summed with the electrons in the calorimeter.

### Bhabha event spectrum

For the reconstruction of the luminosity spectrum from the energy spectrum of the Bhabha scattering events, it is important to take into account the energy dependence of the Bhabha cross section,

$$\mathcal{B}(E_{CM}) = \mathcal{L}(E_{CM}) \frac{\mathrm{d}\sigma_B}{\mathrm{d}E_{CM}} \propto \mathcal{L}(E_{CM})/E_{CM}^2 \tag{3}$$

Since ISR mostly misses the luminometer, the CM energy reconstructed from the detected particles is $E_{CM,rec} < E_{CM}$, and the corresponding spectrum can be represented as a generalized convolution of $\mathcal{B}(E_{CM})$ and the function $\mathcal{I}(x)$ describing the fractional CM energy loss due to the ISR,

$$h(E_{CM,rec}) = \int_0^{E_{max}} \mathcal{B}(E_{CM}) \frac{1}{E_{CM}} \mathcal{I}(\frac{E_{CM,rec}}{E_{CM}})\, \mathrm{d}E_{CM} \tag{4}$$

In the frame of the two-electron system after emission of ISR and before emission of the FSR, i.e. the *collision frame*, the deflection angles in the collision are the same for both particles, according to the momentum-conservation principle. One can, therefore, define a unique *scattering angle* $\theta^{coll}$.[3]

[3]Rigorous definition of the collision frame is not straightforward because of the quantum

## 2.2 Simulation tools for the analysis of the physics of the luminosity measurement

To estimate the precision of the luminosity measurement, Bhabha events in the bunch-collision were simulated using the Guinea-Pig software for the simulation of the bunch crossing [1], and the BHLUMI Bhabha event generator [11]. For details on feeding BHLUMI events to Guinea-Pig, see Ref. [12].

The simulations were run with the standard parameter set from the ILC Technical Progress Report 2011 [13] as the basis for both the 500 GeV and the 1 TeV ILC cases, as well as with the standard simulated bunch density and momentum distributions for CLIC from Ref. [14]. In the ILC case, beside the standard parameter set, simulations were also performed with 24 different variations of individual beam-parameters, in order to determine the influence of the beam-parameter uncertainties on the performance of the presented methods. The simulated beam-parameter variations included symmetric variations of the bunch size parameters $\sigma_{x,y,z}$ and the bunch charge $q$ by $\pm 10$ and $\pm 20\%$, one-sided variations of $\sigma_{x,y,z}$ ans $q$ by $+20\%$, as well as beam misalignment in x- and y-direction by up to one $\sigma_{x,y}$, respectively.

The interaction with the detector was approximated by parametrization of the detector resolutions, as well as by summing together the four-momenta of all particles that are closer together than one Molière radius, as described in detail in Ref. [12].

# 3 Correction of the beam-beam effects

The analysis of the Bhabha count proceeds as follows: correction of the angular counting loss, deconvolution of the ISR energy loss, numerical correction for the counting bias due to the LumiCal energy resolution [12], and finally the correction of the EMD counting bias.

## 3.1 Angular counting loss

Since the angles of the detected showers, $\theta_1^{lab}$ and $\theta_2^{lab}$, are boosted by $\vec{\beta}_{coll}$ with respect to the scattering angle $\theta_{coll}$, $\vec{\beta}_{coll}$ can be reconstructed to a good approximation from $\theta_1^{lab}$ and $\theta_2^{lab}$. If $\beta_{coll}$ is taken to be collinear with the $z$-axis, the

interference between ISR and FSR. In practice, the collision frame is defined as the CM frame of the final electrons together with all radiation within a given tollerance angle with respect to the respective final electron momenta.

system of two equations given by the expressions for the boost of the final particle momenta allows reconstructing $\beta_{coll}$ and $\theta_{coll}$,

$$\beta_{coll} = \frac{\sin(\theta_1^{lab} + \theta_2^{lab})}{\sin\theta_1^{lab} + \sin\theta_2^{lab}} \quad ; \quad \frac{1}{\tan\theta_{coll}} = \gamma_{coll}\left(\frac{1}{\tan\theta_1^{lab}} - \beta_{coll}\frac{1}{\sin\theta_1^{lab}}\right) \tag{5}$$

The effective acceptance of Bhabha events in the luminometer decreases with increasing $\beta_{coll}$. The effective limiting scattering angles $\theta_{min}^{coll}$ and $\theta_{max}^{coll}$ in the collision frame for a given $\beta_{coll}$ are obtained by boosting $\theta_{min}$ and $\theta_{max}$ into the collision frame. This allows calculating the event-by-event weighting factor to compensate for the loss of acceptance,

$$w(\beta_{coll}) = \frac{\int_{\theta_{min}}^{\theta_{max}} \frac{d\sigma}{d\theta}\, d\theta}{\int_{\theta_{min}^{coll}}^{\theta_{max}^{coll}} \frac{d\sigma}{d\theta}\, d\theta}. \tag{6}$$

The results of correction are shown in Fig. 3 for the 1 TeV case. The control spectrum (black) contains all events that would hit the FV of the LumiCal if there were no boost of the collision frame. The detected spectrum is shown in red, and the corrected spectrum green. The blue line represents the events for which $\beta_{coll}$ is higher than some limiting value $\beta^*$, at which the effective acceptance of LumiCal is reduced to zero. Due to kinematic constraints, high values of $\beta_{coll}$ are possible only with high energy loss, which explains the sudden drop of such events at 80% of the nominal CM energy. However, a small number of events with apparent $\beta_{coll} > \beta^*$ is present also at energies above 80% of the nominal CM energy, because occasionally the assumption that $\beta_{coll}$ is collinear with the beam axis is broken due to off-axis ISR. This is visible in the zoomed figure (Fig. 3, right), where these events are scaled by a factor 100.

The following is the list of sources of systematic uncertainty of the collision-frame method:

1. Off-axis ISR. In rare events with significant off-axis ISR, the assumption that $\beta_{coll}$ is collinear with the beam axis does not hold,

2. The implicit assumption that the cluster around the most energetic shower always contains the Bhabha electron. In a fraction of events of the order of a few permille, this is not the case, and the reconstructed polar angles $\theta_{1,2}^{lab}$ may differ from the final electron angles.

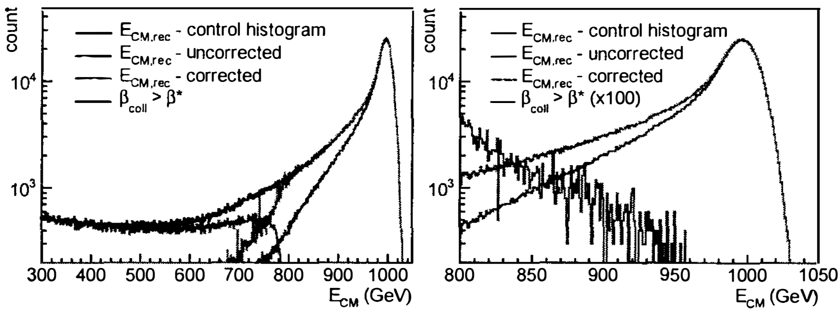


Figure 3: Correction of the counting loss due to Beamstrahlung and ISR at 1 TeV. Left: whole spectrum; right: zoom on energies above 800 GeV. Black: Simulated control spectrum without counting loss due to Beamstrahlung and ISR; red: Reconstructed $E_{CM}$ spectrum affected by the counting loss; green: Reconstructed spectrum with correction for the counting loss due to Beamstrahlung and ISR; blue: events inaccessible to the correction

3. The use of the approximate angular differential cross section for the Bhabha scattering in the calculation of the correction weight,

4. Assumption that all ISR is lost, and all FSR is detected, in the calculation of $\beta_{coll}$ and $w$.

The relative bias due to the off-axis ISR is if the order of one permille. This bias is related to the energy- and angular distribution of the ISR, which is reliably predicted by the generator. Thus this bias can be reliably corrected, and it is not sensitive to beam-parameter variations.

The uncertainty introduced by the implicit assumption that the cluster around the most energetic shower always contains the Bhabha electron depends on the beam parameters, and it may even depend on the specifics of the position-reconstruction algorithm in the luminometer. Its correction is beyond the scope of the present study. The contribution of the effects 3 and 4 is smaller than the statistical uncertainty of the present analysis. The final quoted uncertainty, containing the contributions from the effects 2, 3 and 4 in the upper 20% of the luminosity spectrum is as follows: For the 500 GeV ILC, the uncertainty is $(+0.4 \pm 0.1) \times 10^3$, for the 1 TeV ILC, it is $(+0.7 \pm 0.1) \times 10^3$. The absolute size of these final biases can be taken as the present estimate of the uncertainty of the luminosity measurement induced by beamstrahlung and ISR.

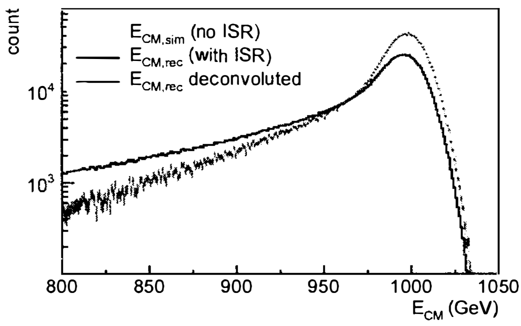


Figure 4: Deconvolution of the ISR deformation of the luminosity spectrum. Yellow: the control histogram – simulated $E_{CM}$ before emission of ISR, smeared with a normalized Gaussian; black: the histogram affected by the ISR energy loss – reconstructed $E_{CM}$ from the detected showers, green: deconvoluted spectrum.

## 3.2 ISR energy loss

To obtain the Bhabha CM energy distribution $\mathcal{B}(E_{CM})$, the ISR energy loss should be deconvoluted from $h(E_{CM,rec})$. This deconvolution can be performed using the theoretical form of the distribution $\mathcal{I}(x)$ of the ISR fractional energy loss, and by solving the system of linear equations resulting from the discretization of Eq. 4 [12]. To obtain the function $\mathcal{I}(x)$, the distribution of $x = E_{CM,rec}/E_{CM}$ was taken from the BHLUMI file, and the beta distribution was fitted to it for $x > 0.8$.

The results of the deconvolution are shown in Fig. 4. The control histogram (yellow) contains simulated CM energies before ISR emission, smeared by the energy resolution of the LumiCal. The histogram with ISR energy loss (black) is simply the histogram resulting from the correction of the angular counting loss in the previous step. The deconvoluted histogram is shown as green points with error bars.

The uncertainty estimate of the deconvolution procedure alone for the integral luminosity in the upper 20% of the spectrum is given by the relative integral difference between the deconvoluted and the control spectrum in the upper 20%. This uncertainty is $(+0.81 \pm 0.22) \times 10^{-3}$ at 1 TeV, and $(+0.35 \pm 0.21) \times 10^{-3}$ at 500 GeV.

## 3.3 Energy resolution

Since full energy information of the detected particles is used to determine the luminosity spectrum, the energy resolution of LumiCal induces a bias in the Bhabha count by asymmetric redistribution of events around the CM energy cut because of the slope in the form of the spectrum at the cut energy. This can be corrected by integration of the fitted parametrized form of $\mathcal{B}(E_{CM})$. When the cut is made at 80% of the nominal energy, the size of this correction is between 1 and $4 \times 10^{-4}$. It has been shown in Ref. [12] that the energy-resolution effect can be corrected to better than $1 \times 10^{-4}$.

## 3.4 Angular loss due to the EMD

The EMD shifts the polar angles of the outgoing particles consistently towards smaller angles. Since the Bhabha cross section is monotonously decreasing with the polar angle, the net effect of the EMD is a decrease in the Bhabha count. Since the EMD bias is small, correction by MC simulation of the bunch crossing has sufficient precision. The precision is limited by the beam-parameter uncertainties in the MC simulation. If the conservative beam-parameter uncertainty described in Sec. 2.2 is taken, the precision of EMD correction is $\pm 5 \times 10^{-4}$ of the total luminosity at 500 GeV, and $\pm 2 \times 10^{-4}$ at 1 TeV. If the beam parameters are known with better precision than 20% (see Ref. [15]), the residual uncertainty will be correspondingly smaller.

# 4 Overview of the systematic uncertainties in luminosity measurement

Beside the uncertainties remaining after correction of the beam-beam effects, a number of further systematic effects limits the achievable luminosity precision at future linear colliders. These will be briefly reviewed here.

## 4.1 Physics background

A major systematic effect in the luminosity measurement originates from the four-fermion neutral-current processes of the type $e^+e^- \to e^+e^-f\bar{f}$. These processes have a signature similar to Bhabha scattering, characterized by the outgoing $e^+e^-$ pairs at low angles carrying a large fraction of the beam energy so they can be miscounted as signal. Using event selection based on coplanarity and CM energy, the fraction is reduced to 2.2 permille at 500 GeV and 0.8 permille at 1 TeV [16].

At present there are no accurate estimates of the theoretical precision with which the fraction of physics background events is calculated. Thus the above quoted fractions, obtained using the WHIZARD generator, will be taken as a full-size effect.

## 4.2 Systematics of the polar angle reconstruction

Matching of the experimental and the theoretical selection cuts in Eq. 2 depends crucially on the precision of the reconstruction of the polar-angle of the shower.

**The inner radius** of the active volume of the LumiCal has to be known with precision of 10 $\mu m$ in order to keep the resulting luminosity uncertainty well below 1 permille [17, 18].

**Position uncertainty LumiCal – IP** reflects directly on the polar angle uncertainty. It is affected by the lateral positioning uncertainty of the Lumical relative to the final beam-delivery quadrupole, by the uncertainty of the lateral IP position determined by the beam-position monitors, and by the longitudinal uncertainty in the relative positioning of the two calorimeters. All three of these parameters must be known at the level of several hundred $\mu m$ in order to keep the resulting luminosity uncertainty at the one-permille level [17, 18].

**Intrinsic reconstruction uncertainties** due to the shower reconstruction algorithm of the LumiCal introduce a polar angle bias of $3.2 \times 10^{-3}$ mrad and polar angle resolution of $2.2 \times 10^{-2}$ mrad [19]. Each of these effects adds an independent contribution of 0.16 permille to the luminosity uncertainty [17].

## 4.3 Cross section

The Bhabha cross-section calculation for the LEP experiment reached a precision of 0.54 permille [6]. For the future linear colliders, new calculations are necessary, because the contribution of the virtual $Z$-boson exchange alters the cross section significantly. Presently a new Bhabha generator is under development [20] which will include beam polarization, the background processes, as well as the wide-angle measurement.

The uncertainty on the beam polarization affects the luminosity figure via the cross-section calculation at the level of 0.19 permille [17].

# 5 Conclusions

Precise luminosity measurement is essential at linear colliders in order to fully exploit their intrinsic precision physics capabilities. A number of systematic effects, of whoch the most dramatic are the beam-beam effects, limit the achievable precision.

The collision-frame method corrects the beam-beam effects by directly measuring the counting losses via experimentally observable quantities related to the beam-beam effects in a fundamental way. Precision of below 1 permille is reached, essentially independent of the precision with which the key beam parameters are known.

Contributions of the beam-beam effect correction, as well as from other sources, to the overall systematic uncertainty of the luminosity measurement are listed in Tab. 1.

Table 1: Systematic uncertainties in luminosity measurement.

| Source of uncertainty | 500 GeV ($10^{-3}$) | 1 TeV ($10^{-3}$) |
|---|---|---|
| Bhabha cross section | 0.54 | 0.54 |
| Polar-angle resolution | 0.16 | 0.16 |
| Polar-angle bias | 0.16 | 0.16 |
| IP lateral position | 0.1 | 0.1 |
| Energy resolution | 0.1 | 0.1 |
| Energy scale | 1 | 1 |
| Beam polarization | 0.19 | 0.19 |
| Correction of angular losses due to Beamstrahlung | 0.4 | 0.7 |
| ISR deconvolution | 0.4 | 0.8 |
| EMD correction | 0.5 | 0.2 |
| Physics background | 2.2 | 0.8 |
| Total | 2.6 | 1.8 |

The final uncertainty is 2.6, respectively 1.8 permille in the 500 GeV and the 1 TeV cases. This satisfies the requirement for the largest part of the Physics programme at the ILC. However, for high-precision measurements such as the Giga-Z programme, precision of $10^{-4}$ is required [21]. Uncertainties presented here may be refined towards this goal as more precise knowledge becomes available on beam-parameter physical correlations, the cross section of the physics background, as well as with further refinement of the correction methods.

# References


[1] D. Schulte, *Study of Electromagnetic and Hadronic Background in the Interaction Region of the TESLA Collider.* PhD thesis, Hamburg University, 1996.

[2] F. Simon, *Optimum lumi spectrum and required accuracy for a tt scan near threshold*, in *FCAL workshop, DESY Zeuthen, Germany*, 7-9 May, 2012. https://indico.desy.de/conferenceDisplay.py?confId=5333.

[3] OPAL Collaboration, *Eur.Phys.J.* **C14** (2000) 373–425, [hep-ex/9910066].

[4] **ALEPH Collaboration** Collaboration, ALEPH Collaboration, *Eur.Phys.J.* **C14** (2000) 1–50.

[5] **L3 Collaboration** Collaboration, L3 Collaboration, *Eur.Phys.J.* **C16** (2000) 1–40, [hep-ex/0002046].

[6] A. Arbuzov et al., *Physics Letters B* **383** (1996) 238.

[7] ILC Collaboration, *The International Linear Collider - Technical Design Report.* International Linear Collider, 2013. ILC-REPORT-2013-040, http://www.linearcollider.org/ILC/TDR.

[8] M. Aicheler et al., eds., *A multi-TeV linear collider based on CLIC technology: CLIC Conceptual Design Report.* CERN European organization for nuclear research, 2012. CERN-2012-007.

[9] C. Rimbault, P. Bambade, K. Mönig, and D. Schulte, *Journal of Instrumentation* **2** (2007) P09001.

[10] K. Yokoya and P. Chen, *Beam-beam phenomena in linear colliders*, in *Frontiers of Particle Beams: Intensity Limitations*, vol. 400 of *Lecture Notes in Physics*, pp. 415–445, Springer Verlag, 1991. US-CERN School on Particle Accelerators.

[11] S. Jadach, W. Placzek, E. Richter-Was, B. Ward, and Z. Was, *Computer Physics Communications* **102** (1997) 229.

[12] S. Lukić, I. Božović-Jelisavčić, M. Pandurović, and I. Smiljanić, *Journal of Instrumentation* **8** (2013) P05008, [arXiv:1301.1449]. LCD-Note-2012-008.

[13] E. Elsen et al., eds., *International Linear Collider - A technical progress report*. International Linear Collider, 2011. ILC-REPORT-2011-30, ISBN: 978-3-935702-56-0.

[14] D. Schulte et al., *CLIC simulations from the start of the linac to the interaction point*, in *Proceedings of EPAC 2002, Paris, France*, 2002. CERN-PS-2002-053-AE ; CLIC-Note-529.

[15] C. Grah and A. Sapronov, *Journal of Instrumentation* **3** (2008), no. 10 P10004.

[16] I. Božović-Jelisavčić, S. Lukić, G. Milutinović-Dumbelović, M. Pandurović, and I. Smiljanić, *Journal of Instrumentation* **8** (2013) P08012, [arXiv:1304.4082].

[17] H. Abramowicz et al., *Journal of Instrumentation* **5** (2010) P12002.

[18] A. Stahl, *Luminosity measurement via Bhabha scattering: Precision requirements for the luminosity calorimeter*, LC Note LC-DET-2005-004, SLAC, 2005.

[19] I. Sadeh, *Luminosity measurement at the International Linear Collider*, Master's thesis, Tel Aviv University, 2008.

[20] V. Makarenko, *New generator for Bhabha scattering*, in *The XII-th International School-Seminar, The Actual Problems of Microworld Physics, Gomel, Belarus*, July 22 - August 2, 2013.

[21] T. Behnke, C. Damerell, J. Jaros, and A. Miyamoto, eds., *International Linear Collider - Reference Design Report*, vol. 4. ILC Global Design Effort and World Wide Study, 2007.